Blow-up overheating instability in vanadium dioxide thin films

V. I. Polozov,[1,2] S. S. Maklakov,[1,2] A. L. Rakhmanov,[1,2] S. A. Maklakov,[1] and V. N. Kisel[1]
[1]*Institute for Theoretical and Applied Electromagnetics, Russian Acad. Sci., Moscow, 125412, Russia*
[2]*Moscow Institute of Physics and Technology, Dolgoprudnyi, Moscow Region, 141700, Russia*

(Received 17 March 2020; revised manuscript received 1 June 2020; accepted 16 June 2020; published 26 June 2020)

We study an insulator-metal transition (IMT) in vanadium dioxide films. We argue that the main features of the voltage-induced IMT in these systems can be understood within a theory of the blow-up overheating instability. In the blow-up regime, the IMT occurs locally even in uniform films: a narrow "hot" metallic channel along the current direction arises in the insulating "cool" environment. We derive an instability criterion and analytical formulas for a characteristic instability time and the hot-channel width. We apply our results to the experiments on the epitaxial films available in the literature and our measurements performed on the specially prepared VO_2 granular films. The main features of the voltage-induced IMT are the same for all considered samples and can be described in the framework of the proposed theory. Interestingly, the mathematical description of the voltage-induced IMT in the vanadium oxide is similar to that proposed for the superconductor-normal state transition in high-T_c tapes. However, the hot channel in high T_c is directed across the current flow, while in the case of the IMT it is directed along the current.

DOI: 10.1103/PhysRevB.101.214310

I. INTRODUCTION

A number of intriguing dynamical processes in plasmas, semiconductors, and superconductors can be described in terms of the overheating instability and blow-up regime [1–5]. Such phenomena were investigated in applied mathematics and it was found that they obey rather general features, independent of the physical nature of the particular system [6]. Here we apply such an approach to describe experimental observations of the voltage-induced insulator-metal transition (IMT) occurring in thin films of VO_2 [7–10]. We find the instability criterion, which properly describes the experiments. We show that the IMT should occur locally even in a homogeneous film due to heat localization, a phenomenon characteristic of the blow-up regimes. The heat localization gives rise to the formation of thin hot metallic channels in a cool insulating ambient directed along the transport current flow. We derive analytical expressions for the characteristic time of raising the voltage-induced IMT and the spatial scale of the high-conductivity channel that nucleates in the initially insulating film. We also suggest analytical expressions to describe the time dynamics of the instability at the initial stage. We compare the obtained theoretical results with the experiments taken from literature and our own and find a good agreement between calculated and measured quantities. Interestingly, in general features, a similar mechanism allows describing the superconducting–normal state transition in high-T_c superconductors [11,12]. However, in the latter case the hot normal channel nucleates across the current flow.

The problem of the IMT in VO_2 includes two aspects: microscopic (see, e.g., [13]) and macroscopic. The microscopic aspect of the problem is a separate task, which is of interest and importance. It is one of the classical problems of the systems with strongly correlated electrons [14]. However, there is no commonly accepted explanation of the IMT in vanadium oxides [15].

Here we consider only the macroscopic part of the problem. Thus, we do not discuss the physical nature of the IMT itself. The microscopic properties of the system are responsible for the appearance of the observed resistance versus temperature dependence $R(T)$. In our macroscopic treatment we need only $R(T)$ and threshold values of the voltage and temperature, at which voltage-induced IMT occurs. The overheating mechanism of the voltage-induced IMT in oxide films was suggested in several papers starting from Ref. [7] and developed in further studies (see, e.g., Refs. [16–18]). Our goal is *to explain from a general point of view* an intriguing feature that is observed in many experiments (see, e.g., [19]): a nonhomogeneous development of the overheating in homogeneous samples. For this purpose we take for a comparison results obtained for two types of samples. The first are the data for high quality epitaxial VO_2 films from Ref. [7]. The second are the results obtained in our experiments with nanocrystalline granular VO_2 films. These locally inhomogeneous films were sputter-deposited intentionally for the purpose of the present study. We observed that the qualitative picture of the IMT is the same in the media with different local homogeneity. We also obtain analytical estimates for characteristic transition parameters and demonstrate that the voltage-induced IMT in VO_2 samples can be described within the theory of blow-up overheating instability.

The paper is organized as follows. In Sec. II we describe our experimental procedures and the main features of the IMT observed in VO_2 thin films. In Sec. III we formulate a mathematical model of the problem, present the results of our calculations, and compare them with experimental observations. In Sec. IV we discuss the obtained results.

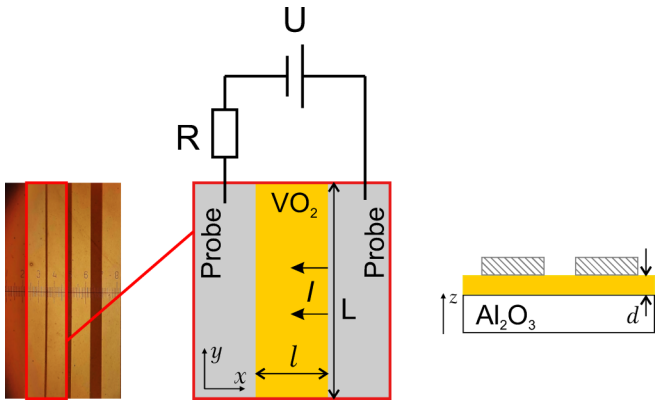

FIG. 1. The geometry of the experiment: $L = 2$ mm, $d =$ 130 nm, and VO_2 channel length $l = 10$ μm. The resistor prevents damage of the device caused by the sample's steep resistance change during the IMT.

II. EXPERIMENT AND RESULTS

We performed our experiments using specially prepared granular VO_2 films. This was done to ensure that the voltage-induced IMT in the vanadium oxide film is independent of its local structure.

The films of VO_2 with a thickness of 130 nm were deposited by rf-magnetron sputtering of V target on poly-crystalline Al_2O_3 substrate with post-deposition annealing. Sputtering was carried out in a mixture of high purity Ar (99.999%) and O_2 with a total pressure of 1 mTorr. Oxygen concentration was optimized to 13.5 vol. %. The Al_2O_3 substrate temperature was 400 °C during deposition. The deposition time was 30 min. After sputtering, the films were annealed at 720 °C in a tube furnace in Ar flow with a rate of 2000 cm/s for 1 h. The additional details of the deposition process, such as the substrate biasing, the target-substrate distance, etc. are described in Ref. [20].

The layer of Ni with a thickness of 130 nm was deposited by the DC magnetron sputtering on the VO_2 films to form electrodes. The electrodes with dimensions 0.5×2 mm were patterned using positive-resist photolithography to form a 10 μm channel of VO_2 in between, see Fig. 1.

Morphological properties of the VO_2 thin films were examined by scanning electron microscopy (SEM) and atomic force microscopy (AFM) (Fig. 2).

The dependence of the resistance R on the temperature T of the sample was measured in a two-probe configuration using the Solartron SI 1287 potentiostat. The sample in series with a shunt resistor was connected to a voltage source as shown in Fig. 1. To obtain $R(T)$, the samples were continuously heated or cooled with a 2 °C/min rate. The 1-V bias was applied to the probes on the sample and the resistance of the sample was recorded two times per second. As usual for the IMT [7], the curves $R(T)$ have a hysteresis (Fig. 3): in the vicinity of the IMT the resistance during heating is larger than the resistance under cooling.

The current-voltage $[I(U)]$ curves were measured under slowly ramping up voltage while keeping the substrate temperature fixed. The voltage and current were recorded using multimeters.

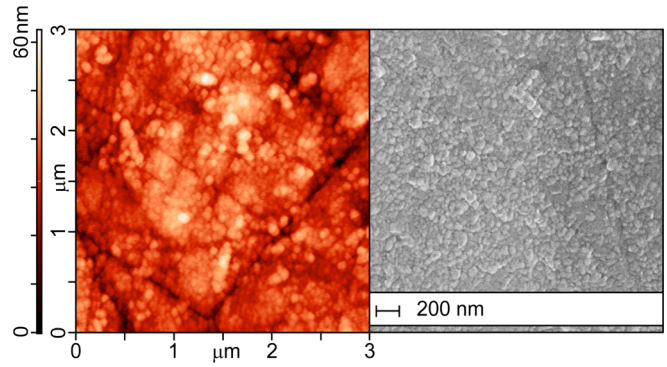

FIG. 2. AFM (a) and SEM (b) images of our VO_2 thin films with granular structure.

The measured $R(T)$, shown in Fig. 3(a), was used to find characteristic parameters of the IMT: amplitude of IMT (the ratio of the resistance in the insulating state to the resistance in the metal state) and transition temperature. In Fig. 3(a) we also show derivatives $d\log[R(T)]/dT$ for both branches of

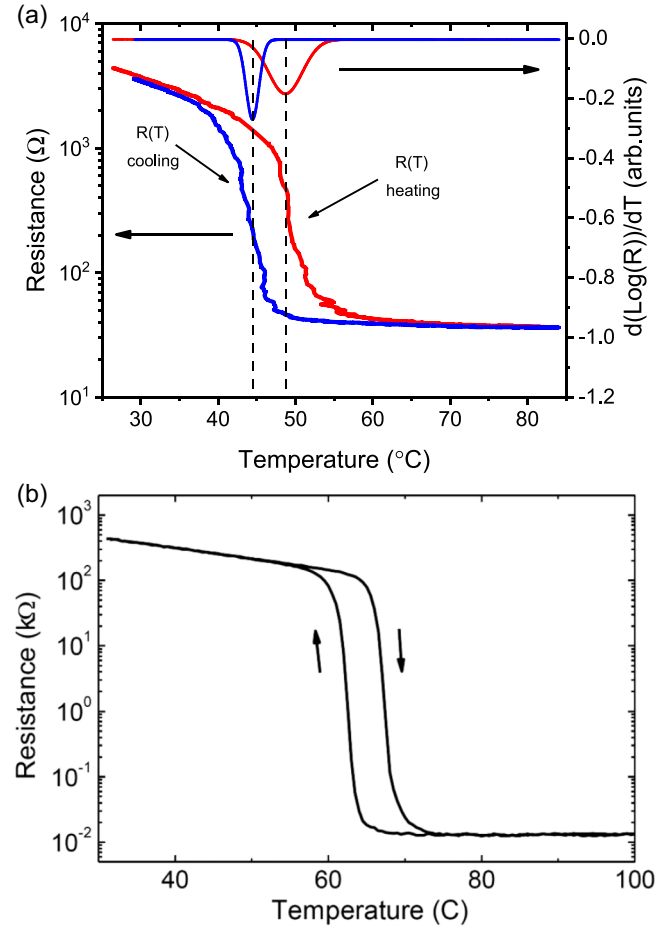

FIG. 3. The $R(T)$ dependence of the granular VO_2 thin film measured in our experiments (a). The dash lines indicate the transition temperatures for heating (T_t) and cooling regimes. The experimental data in (b) are taken from Ref. [7] for high-quality epitaxial films. (Reprinted with permission from [7]. Copyright 2020 by the American Physical Society.)

the hysteresis loop. These values were used to determine the transition temperature (T_t) of the thin film. Note, the parameters of the IMT strongly depended on the film's morphology and crystal structure. The transition temperature of the films obtained here was 49 °C with the IMT amplitude of 10^2. In contrast, for the epitaxial homogeneous VO_2 thin films deposited on the sapphire substrate, the transition temperature is usually about 62-68°C with the amplitude of more than 10^4 (see, e.g., Refs. [7,10,21]). According to SEM and AFM measurements (Fig. 2), our films consisted of grains with a typical size 100 nm. The presence of grain boundaries and crystal imperfections results in the internal stress, which influences the IMT parameters [20]. For comparison, the curve $R(T)$ for high-quality epitaxial VO_2 film taken from Ref. [7] is presented in Fig. 3(b).

The voltage-current curves of the sample recorded under increasing voltage at different fixed temperatures are shown in Fig. 4(a) for our samples and in Fig. 4(b) for the epitaxial film from Ref [7]. The $I(U)$ curves were used to find the threshold voltage of the voltage-induced IMT. Appearance of the curves is typical for the IMT. First, $I(U)$ smoothly grows and the curve is nonlinear since the sample is in the insulating state. Then, at some threshold voltage (U_q), the current flow becomes unstable and the voltage abruptly decreases. Finally, the current rapidly and linearly increases with voltage, which indicates that the sample is now in the metallic state and its resistivity is much lower than before the IMT. The U_q decreases with the growth of T. The authors of Ref. [7] have ascribed this effect to a thermal instability and proved it by direct measurement of the local temperature. The detailed study of the samples in Ref. [7] reveals that the IMT occurs first locally in a rather narrow hot channel while the remaining sample volume is still insulating. A uniform metallic state arises in the film at the second stage of the IMT.

From the results shown in the figures above, we see that the qualitative pictures of the IMT in the granular and epitaxial films are quite similar, despite differences in the values of the characteristic parameters of the IMT. Thus, we conclude that a macroscopic mechanism of the IMT in the vanadium dioxide films is universal and independent of the film structure. Here we present a detailed analysis of the IMT in terms of the thermal instability.

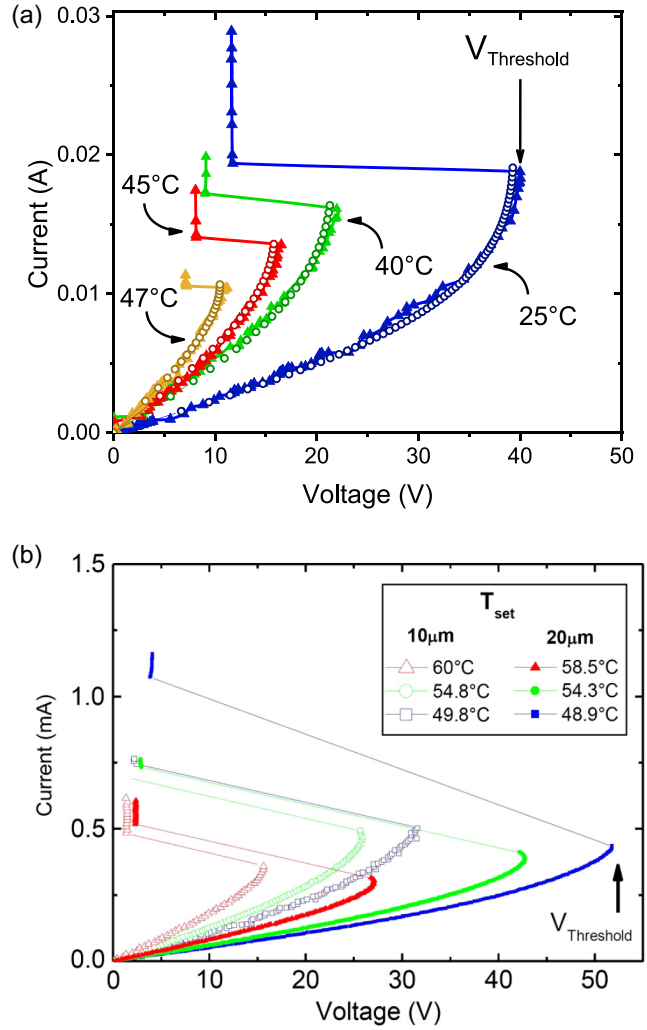

FIG. 4. The experimental (triangle dots) and theoretical (hollow circular dots) $I(U)$ curves of our VO_2 films at various ambient temperatures (a). The theoretical curves are obtained using Eq. (6). The experimental curves for the samples from Ref. [7] are shown in (b). The $I(U)$ curves in (b) are measured on epitaxial samples with VO_2 channel length l of 10 and 20 μm. (Reprinted with permission from [7]. Copyright 2020 by the American Physical Society.)

III. MODEL AND CALCULATIONS

We analyze a usual experimental geometry (see, e.g., Ref. [7]), which is shown schematically in Fig. 1: an insulating film of the vanadium dioxide at temperature T near the IMT transition temperature is placed between two electrodes. A voltage U is applied across the film (along the x axis). The film thickness d is much less than its width l and length L. The film is an insulator at lower temperatures, while at higher temperatures it is a metal.

We write down a standard heat equation for T in the form

$$C\dot{T} = \nabla[\kappa\nabla T] + Q(T, \mathbf{r}), \tag{1}$$

where C and κ are the heat capacity and heat conductivity, $Q(T, \mathbf{r})$ is the Joule heat per unit volume, and $\mathbf{r} = (x, y, z)$ is a coordinate. The boundary conditions at the film surface are

$$-\kappa(\nabla T)_{\mathbf{n}} = q(T, T_s), \tag{2}$$

where $(\nabla T)_{\mathbf{n}}$ is the temperature gradient along the normal $\mathbf{n}$ to the film surface, q is the heat flux from the film to the ambient, and T_s is the ambient temperature. The initial condition is $T(t = 0, \mathbf{r}) = T_s$. To solve Eq. (1) with boundary conditions Eq. (2) we can use several natural simplifications.

We are interested in a narrow temperature range, where the function $R(T)$ is very steep due to the IMT. Thus, we can neglect the temperature dependence of the heat capacity and the heat conductivity, assuming further that $C = C(T_s)$ and $\kappa = \kappa(T_s)$. The main heat removal from the sample occurs due to the substrate and to the electrodes. The length of the electrodes L is much larger than l and d. Under such conditions, the temperature change in the x and z directions is small, $T(\mathbf{r}) \approx T(y)$, and we can integrate Eqs. (1) and (2)

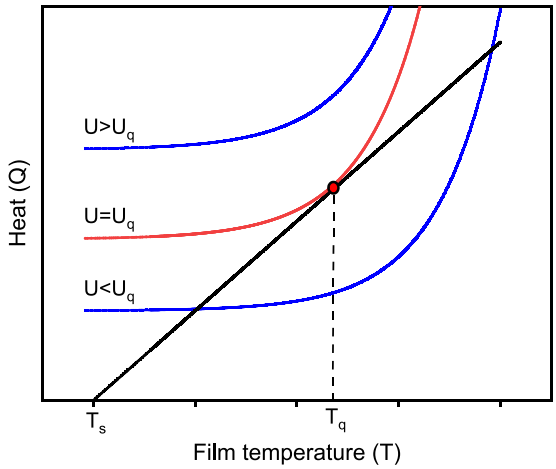

FIG. 5. Stability analysis of the uniform temperature distribution. The blue and red curves show the temperature dependence of the Joule heat near the IMT at different voltages U. The black curve $W = q(T, T_s)/d$ shows the heat removal. The uniform temperature distribution is stable if $U < U_q$, and unstable if $U > U_q$. The red curve at $U = U_q$ is the boundary between stable and unstable regimes.

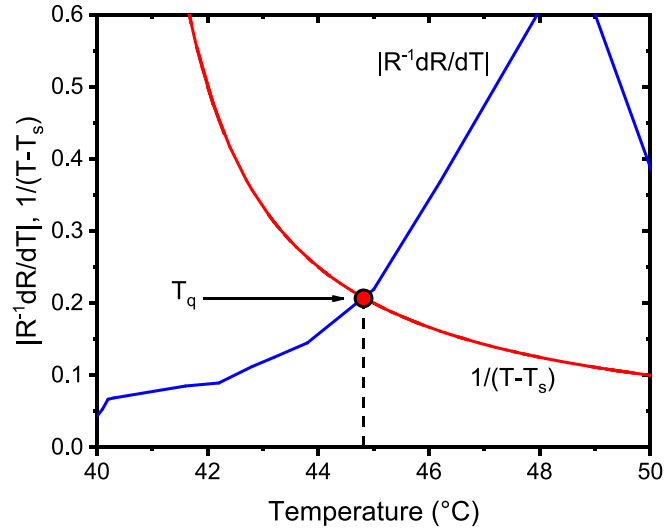

FIG. 6. The value of $|R^{-1}dR/dT|$ versus T is shown as the blue curve. It was calculated using the experimental data for our VO_2 film presented in Fig. 3(a). The red curve is the calculated value of $1/(T - T_s)$ with $T_s = 40\,^{\circ}\mathrm{C}$.

over x and z. As a result, we obtain a usual one-dimensional heat equation

$$C\dot{T} = \kappa \frac{\partial^2 T}{\partial y^2} + Q(T) - q(T, T_s)/d. \tag{3}$$

The applied voltage U induces the current $I = U/R(T)$. Then, the Joule heat release per unit volume is $Q = UI/dlL = E^2/\rho(T)$, where $E = U/l$ is the electric field and $\rho(T) = R(T)dL/l$ is the resistivity.

A. Thermal instability criterion

The stationary and uniform temperature is determined by the condition $Q(T) = q(T, T_s)/d$, see Fig. 5. The solution of the latter equation exists only if the applied voltage is lower than a threshold (quench) value $U_q = E_q l$. This critical voltage and corresponding maximum stable temperature T_q are determined by an additional condition $dQ/dT = (dq/dT)d^{-1}$.

Since we are interested in the narrow temperature range around the IMT, we can expand the function $q(T, T_s)$ in series of $(T - T_s)$: $q(T, T_s)/d = h_0 + h(T - T_s) + h_1(T - T_s)^2 + \cdots$. The first term is zero since there is no heat removal in the thermal equilibrium. We take into account only the linear term, assuming that $h(T - T_s) \gg |h_1|(T - T_s)^2$. This is a standard approximation for the heat removal in thermodynamics and h is frequently referred to as the heat transfer coefficient. Under this approximation, the conditions determining the quenching point (E_q, T_q) have a form

$$\frac{E_q^2}{\rho(T_q)} = h(T_q - T_s),$$
$$-\frac{E_q^2}{\rho^2(T_q)}\left(\frac{d\rho}{dT}\right)_{T_q} = h. \tag{4}$$

If we divide the second equation by the first one, we obtain a formula independent of the unknown value h,

$$\left|\frac{1}{R}\frac{dR}{dT}\right|_{T_q} = \frac{1}{T_q - T_s}. \tag{5}$$

The latter equation can be used to verify whether the overheating instability occurs during the IMT. For this aim, we can calculate the value of $R^{-1}dR/dT$ as a function of T, using the experimental data shown in Fig. 3(a). The results of such calculations are presented in Fig. 6 by a $R^{-1}dR/dT$ curve. Afterward, we specify the ambient temperature T_s and calculate the function $1/(T - T_s)$, shown as a corresponding curve in Fig. 6. The intersection of the curves occurs at $T = T_q$ as it follows from Eq. (5). If we know T_q, we can find $R_q = R(T_q)$ using again the experimental data [Fig. 3(a)]. The results of such calculations for different T_s are shown in Fig. 7 by green open triangles. The experimental value of $R_q = U_q/I_q$ can be obtained from measured voltage-current characteristics, Fig. 4(a). The values U_q and I_q are determined at the disruption points in the $I(U)$ curves. The results are shown in Fig. 7 by green open circles. We assumed that the IMT mechanism in granular films obtained here and epitaxial films from Ref. [7] are the same. In order to confirm this, we can do the same procedure for a 10 μm channel and a 20 μm channel of epitaxial VO_2 films using experimental data from Ref. [7] [Figs. 3(b) and 4(b)]. We have to take into account that the resistance R for a 10 μm channel is twice smaller than that for the 20 μm channel. The results are presented in Fig. 7 by red and blue open triangles [calculations according to Eq. (5)] and circles [experimental, Fig. 4(b)]. As it is seen from Fig. 7, the theory and experiment are in a good quantitative agreement.

We can calculate theoretically the $I(U)$ curves for our samples using determined above quenching parameters (U_q, T_q, R_q) and measured $R(T)$. First, we find the uniform stationary temperature of the sample T at applied voltage U

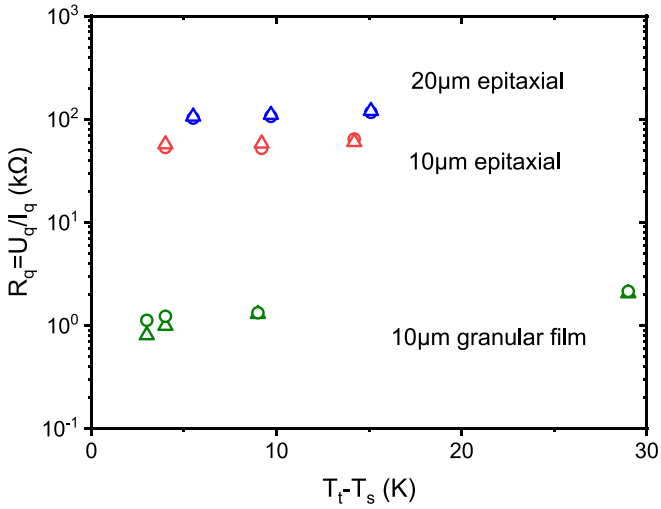

FIG. 7. The quenching resistance R_q versus the difference between transition temperature T_t in the heating regime (see Fig. 3) and T_s. The measured transition temperature for our granular films is 49 °C and T_t of the epitaxial films from Ref. [7] is 69 °C. The open circles show experimental data for VO_2 films. The open triangles show the R_q calculated using Eq. (5).

using the condition $Q(T) = q(T, T_s)/d = h(T - T_s)$, where $Q = U^2/R(T)dlL$. The heat transfer coefficient h we exclude from equations using the first of Eqs. (4). As a result, we relate the film temperature T and U:

$$U^2 = \frac{R(T)U_q^2(T - T_s)}{R_q(T_q - T_s)}. \tag{6}$$

We substitute in this equation the measured resistance $R(T)$ [Fig. 3(a)] and solve Eq. (6) numerically. With known T and U, we find I as $I = U/R(T)$. The calculated curves $I(U)$ are shown in Fig. 4(a) by open circles. The agreement between the experimental and theoretical results is quite well, which confirms the overheating nature of the instability.

B. Instability development and heat localization

The next intriguing feature of the observed voltage-induced IMT is the local character of the transition nucleation [7,8]. The IMT occurs first within a narrow "hot" channel along the direction of the current flow, while the remaining sample is in the insulating "cold" phase. We show that this feature is an inherent property of the overheating instability in the geometry studied and does not require any additional suggestions about film homogeneity, e.g., due to electronic phase separation [22,23].

Let us expand the difference $Q(T) - q(T, T_s)/d$ in a series in $(T - T_q)$ near T_q. Taking into account Eqs. (4) we derive

$$Q(T) - \frac{q(T, T_s)}{d} = \frac{(T - T_q)^2}{2}\left[E_q^2\sigma''(T_q) - \frac{q''(T_q)}{d}\right], \tag{7}$$

where $\sigma = \rho^{-1}$ is the conductivity, and $f''(T_q)$ means the second derivative of the function with respect to the temperature, taken at the "quench" point $T = T_q$. We analyze the processes near the IMT, where the conductivity varies very fast, while the change of the heat transfer is not so strong. Then, we can assume that the second term in the square brackets in Eq. (7) is smaller than the first one and can be neglected. Substituting Eq. (7) in the heat equation (3) and introducing dimensionless variables we obtain

$$\frac{\partial\theta}{\partial\tau} = \frac{\partial^2\theta}{\partial\xi^2} + \alpha\,\theta^2, \tag{8}$$

where

$$\theta = \frac{T - T_q}{T_q - T_s}, \quad \tau = \frac{t}{t_0}, \quad \xi = \frac{y}{y_0}, \quad y_0^2 = \frac{\kappa t_0}{C},$$
$$\alpha = E_q^2\,\sigma''(T_q)\frac{(T_q - T_s)\,t_0}{C}. \tag{9}$$

Later on we will determine the value of the characteristic time t_0.

Equations of the type of Eq. (8), $\dot\theta = \theta'' + \alpha\theta^\beta$, are well known in applied mathematics. In particular, if $\beta > 1$, their homogeneous solution and any solution, which decays at $\xi \to \infty$, are unstable with respect to the (local) blow-up instability [6]. The physical reasons for the instability localization could be understood as follows. Assume that the temperature increases in some place of the film. Thus, the resistivity there decreases and, at the fixed voltage, the current density and, consequently, the Joule heat also increases in that location. This, in turn, gives rise to further heating (positive feedback), and so on. However, if $\beta > 1$ the local increase of the temperature is so fast that ambient regions of the sample remain almost unperturbed.

Equation (8) can be solved numerically. However, it is much more insightful to find analytical results that allow us to estimate the characteristic width of the overheated channel and the time of the instability development.

We assume that some thermal perturbation (due to thermal fluctuations or some small inhomogeneity) occurs at $\xi = 0$. We will search for a solution to Eq. (8), which is symmetric with respect to $\xi = 0$ and decaying when $\xi \to \infty$. Such a solution unambiguously goes to infinity in a finite time, as was stated above. To obtain the result of the desired type we introduce the function G, which is related to the dimensionless temperature θ by the equation $\theta = G/(1 - \tau)$ and will seek a self-similar solution G of Eq. (8) depending only on a new variable $\eta = \xi/\sqrt{1 - \tau}$. As a result, Eq. (3) is rewritten as

$$G'' - \frac{\eta}{2}G' - G + \alpha G^2 = 0. \tag{10}$$

The boundary conditions to this equation are $G'(0) = G(\infty) = 0$ since $\partial\theta/\partial\xi = 0$ if $\xi = 0$ and $\theta(\infty) = 0$. Let $G(0) = G_0$ and note that $G_0 = \theta(\tau = 0, \xi = 0) = \theta_0$; the value $\theta_0 = (T_0 - T_q)/(T_q - T_s)$ characterizes the initial perturbation. Naturally, instability can occur only if $T_0 > T_q$.

The asymptotic of $G(\eta)$, when $\eta \to \infty$, can be readily obtained: $G = C_1/\eta^2$, where C_1 is constant. At small $\eta \ll 1$ we can neglect the term $\eta G'$. In this limit

$$\frac{G}{G_0} = 1 - \frac{\alpha G_0 - 1}{2}\eta^2, \quad |\eta| \ll 1. \tag{11}$$

We can match two asymptotics at some $\eta = \eta_1$, requiring the continuity of G and G'. Therefore, we find η_1 and obtain the

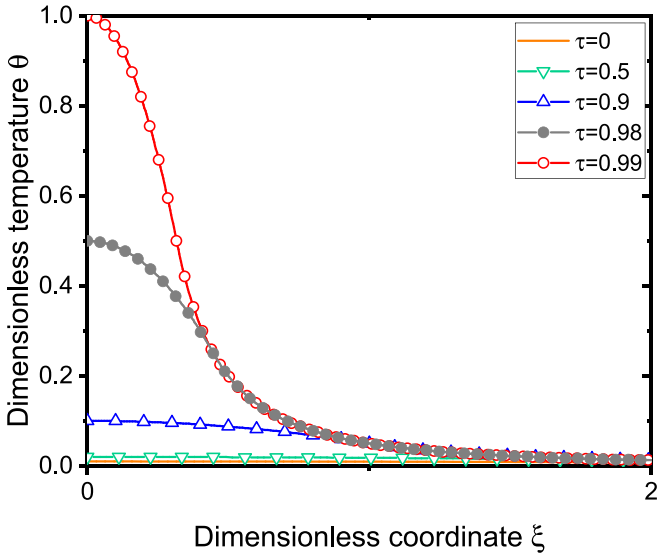

FIG. 8. Dimensionless temperature θ versus coordinate ξ for different times τ [Eq. (12)] with $\theta_0 = 0.01, \alpha = 110$.

approximate solution G of Eq. (10) in the form

$$G(\eta) = G_0 \begin{cases} 1 - \frac{\alpha G_0 - 1}{2}\eta^2, & \eta < \eta_1 = \frac{1}{\sqrt{\alpha G_0 - 1}}; \\ \frac{1}{2(\alpha G_0 - 1)\eta^2}, & \eta > \eta_1. \end{cases} \tag{12}$$

Thus, the dimensionless temperature rise is

$$\theta(\tau, \xi) = \theta_0 \begin{cases} \frac{1}{1-\tau}\left[1 - \frac{(\alpha\theta_0 - 1)\xi^2}{2(1-\tau)}\right], & \xi < \xi_1 = \sqrt{\frac{1-\tau}{\alpha\theta_0 - 1}}; \\ \frac{1}{2(\alpha\theta_0 - 1)\xi^2}, & \xi > \xi_1. \end{cases} \tag{13}$$

It is seen from these equations that the solution that we seek exists only if $\alpha\theta_0 > 1$. The characteristic time t_0 is defined as the time at which the temperature in the overheated region (formally) becomes infinite. It will be estimated self-consistently below.

The time evolution of a small temperature perturbation is illustrated in Fig. 8. As it is seen from the figure, the temperature slowly increases up to τ close to 1. Then, its growth acquires a blow-up appearance. The hot region is localized and its effective size diminishes with time. Such a picture of the overheating process is confirmed by numerical solutions and is typical for blow-up instabilities [6].

We can estimate the value t_0 and a characteristic scale of the hot channel based on the energy conservation law. Let us equate the thermal energy stored in the sample with the total heat release. Such an approach is valid since $\theta'(\xi) \to 0$ when $\xi \to \infty$. Using Eq. (12) for θ, we obtain the following estimates:

$$\int_0^\tau d\tau \int_0^\infty d\xi\, \dot{\theta} \sim \frac{\theta_0}{\sqrt{\alpha\theta_0 - 1}}\left(\frac{1}{\sqrt{1-\tau}} - 1\right),$$
$$\alpha \int_0^\tau d\tau \int_0^\infty d\xi\, \theta^2 \sim \frac{\alpha\theta_0^2}{\sqrt{\alpha\theta_0 - 1}}\left(\frac{1}{\sqrt{1-\tau}} - 1\right). \tag{14}$$

For self-consistency, it is necessary that $\alpha\theta_0 \sim 1$. Thus, using Eqs. (9) we asses the characteristic time and scale of the blow-up instability as

$$t_0 \sim \frac{C}{E_q^2 \sigma''(T_q)(T_0 - T_q)}, \tag{15}$$

$$y_0 \sim \sqrt{\frac{\kappa}{E_q^2 \sigma''(T_q)(T_0 - T_q)}}. \tag{16}$$

According to the experimental data, the characteristic timescale of the IMT lies in the nanosecond range [24–27] and the thickness of the observed hot channels is about several tenths of μm [7,28]. Taking for estimates $E_q = 10^6$ V/m, $\sigma''(T_q) = 10^4$ 1/Ω mK^2, $C = 10^6$ J/m^3 K, and $\kappa = 10$ W/mK, we obtain $t_0 \sim$ 1–10 ns and $y_0 \sim 0.3$–0.1 μm if the initial perturbation is in the range $T_0 - T_q = 0.01$–0.001 K. In our experiment temperature stabilization was about 0.1 K and the latter estimate for possible temperature fluctuations $T_0 - T_q \ll 0.1$ K looks quite reasonable.

IV. DISCUSSION

Thus we show that the voltage-induced insulator-metal transition (IMT) observed in both granular and epitaxial vanadium dioxide thin films can be described in the framework of the overheating instability. The measured and calculated instability thresholds are in a good quantitative agreement. The nonlinearity of the heat release near the IMT gives rise to a blow-up instability. In the blow-up regime, the uniform temperature distribution is unstable with respect to small local perturbations existing either due to the temperature noise or due to some small sample inhomogeneity. For the characteristic parameter values, the timescale of the instability lies in the nanosecond range in agreement with experiment [24–27]), while the spatial scale of the overheated channel is about several tenths of μm, which also agrees with the experiment [7,28]. When the temperature increases, the nonlinearity of the heat release increases. Then, the blow-up mode continues to develop giving rise to the nucleation of a narrow overheated metallic channel in the insulating environment. It is also evident that the thermal noise can lower the "quench" voltage U_q. However, if the noise amplitude ΔT is small, $\Delta T \ll (T_q - T_s)$, the difference between the observed value of voltage of the IMT and U_q is small. The corresponding criterion can be easily derived if necessary.

It is reasonable to assume that characteristic features of the IMT transition could be also described in the framework of the thermal instability, when the current ramps down. For this purpose we can apply $R(T)$ dependence measured under cooling regime, see Fig. 3. However, this effect needs an additional experimental and theoretical investigation. In particular, while the picture of the instability under uniform cooling and heating could be qualitatively similar, the blow-up instability is impossible under current ramp-down regime and, then, the formation of the inhomogeneous current and heat pattern is questionable.

It is interesting to note that the proposed mathematical description of the voltage-induced IMT in the vanadium

oxide is similar to that, which can be used to describe the superconductor-normal state transition in commercial high-T_c tapes [11,12]. However, the hot channel in high-T_c tapes is directed across the current flow in contrast to the IMT where instability develops along the current direction. This difference is due to different I-V regimes of instability in these systems. In the case of the IMT, the instability occurs under fixed voltage conditions (S-shape V-I characteristics), while in the superconductors it occurs under fixed current conditions (N-type I-V characteristics).

ACKNOWLEDGMENTS

The study has been supported by Russian Foundation for Basic Research (RFBR) according to Agreements No. 18-08-00491 and No. 20-52-53020.

[1] X. J. Zhou, Z. S. Gao, L. Han, L. Y. Xiao, T. Hatano, J. Li, D. Koelle, R. Kleiner, H. B. Wang, and P. H. Wu, Hot spot formation in a curved iron-based superconducting whisker, Supercond. Sci. Technol. **32**, 025010 (2019).

[2] A. Doron, I. Tamir, T. Levinson, M. Ovadia, B. Sacépé, and D. Shahar, Instability of Insulators Near Quantum Phase Transitions, Phys. Rev. Lett. **119**, 247001 (2017).

[3] R. G. Mints and A. L. Rakhmanov, Critical state stability in type-II superconductors and superconducting-normal-metal composites, Rev. Mod. Phys. **53**, 551 (1981).

[4] D. V. Denisov, A. L. Rakhmanov, D. V. Shantsev, Y. M. Galperin, and T. H. Johansen, Dendritic and uniform flux jumps in superconducting films, Phys. Rev. B **73**, 014512 (2006).

[5] V. R. Misko, S. Savel'ev, A. L. Rakhmanov, and F. Nori, Negative differential resistivity in superconductors with periodic arrays of pinning sites, Phys. Rev. B **75**, 024509 (2007).

[6] A. A. Samarskii, V. A. Galaktionov, S. P. Kurdyumov, and A. P. Mikhailov, *Blow-up in Quasilinear Parabolic Equations* (Walter de Gruyter, Berlin, New York, 1995).

[7] A. Zimmers, L. Aigouy, M. Mortier, A. Sharoni, S. Wang, K. G. West, J. G. Ramirez, and I. K. Schuller, Role of Thermal Heating on the Voltage Induced Insulator-Metal Transition in VO_2, Phys. Rev. Lett. **110**, 056601 (2013).

[8] J. G. Ramírez, R. Schmidt, A. Sharoni, M. E. Gómez, I. K. Schuller, and E. J. Patiño, Ultra-thin filaments revealed by the dielectric response across the metal-insulator transition in VO_2, Appl. Phys. Lett. **102**, 063110 (2013).

[9] A. S. McLeod, E. Van Heumen, J. G. Ramirez, S. Wang, T. Saerbeck, S. Guenon, M. Goldflam, L. Anderegg, P. Kelly, A. Mueller, M. K. Liu, I. K. Schuller, and D. N. Basov, Nanotextured phase coexistence in the correlated insulator V_2O_3, Nat. Phys. **13**, 80 (2017).

[10] J. del Valle, Y. Kalcheim, J. Trastoy, A. Charnukha, D. N. Basov, and I. K. Schuller, Electrically Induced Multiple Metal-Insulator Transitions in Oxide Nanodevices, Phys. Rev. Appl. **8**, 054041 (2017).

[11] A. L. Rakhmanov, V. S. Vysotsky, and N. V. Zmitrenko, Quench development in long HTS objects—The possibility of "blow-up" regimes and a heat localization, IEEE Trans. Appl. Supercond. **13**, 1942 (2003).

[12] V. Vysotsky, A. Rakhmanov, and N. Zmitrenko, Thermal stability of Bi-2223 wires, in *Research, Fabrication and Applications of Bi-2223 HTS Wires*, World Scientific Series in Applications of Superconductivity and Related Phenomena Vol. 1 (World Scientific, Singapore, 2015), pp. 105–122.

[13] J. Li, C. Aron, G. Kotliar, and J. E. Han, Microscopic theory of resistive switching in ordered insulators: electronic versus thermal mechanisms, Nano Lett. **17**, 2994 (2017).

[14] N. F. Mott, Metal-insulator transition, Rev. Mod. Phys. **40**, 677 (1968).

[15] Z. Yang, C. Ko, and S. Ramanathan, Oxide electronics utilizing ultrafast metal-insulator transitions, Annu. Rev. Mater. Res. **41**, 337 (2011).

[16] V. G. Karpov and D. Niraula, Resistive switching in nanostructures, Sci. Rep. **8**, 12212 (2018).

[17] J. M. Goodwill, A. A. Sharma, D. Li, J. A. Bain, and M. Skowronski, Electro-thermal model of threshold switching in TaO_x-based devices, ACS Appl. Mater. Interfaces **9**, 11704 (2017).

[18] J. M. Goodwill, G. Ramer, D. Li, B. D. Hoskins, G. Pavlidis, J. J. McClelland, A. Centrone, J. A. Bain, and M. Skowronski, Spontaneous current constriction in threshold switching devices, Nat. Commun. **10**, 1628 (2019).

[19] I. Valmianski, P. Y. Wang, S. Wang, J. G. Ramirez, S. Guénon, and I. K. Schuller, Origin of the current-driven breakdown in vanadium oxides: Thermal versus electronic, Phys. Rev. B **98**, 195144 (2018).

[20] S. S. Maklakov, V. I. Polozov, S. A. Maklakov, A. D. Mishin, I. A. Ryzhikov, A. L. Trigub, V. A. Amelichev, K. I. Maslakov, and V. N. Kisel, Post-deposition annealing of thin RF magnetron sputter-deposited VO_2 films above the melting point, J. Alloys Compd. **763**, 558 (2018).

[21] A. M. Makarevich, I. I. Sadykov, D. I. Sharovarov, V. A. Amelichev, A. A. Adamenkov, D. M. Tsymbarenko, A. V. Plokhih, M. N. Esaulkov, P. M. Solyankin, and A. R. Kaul, Chemical synthesis of high quality epitaxial vanadium dioxide films with sharp electrical and optical switch properties, J. Mater. Chem. C **3**, 9197 (2015).

[22] E. Dagotto, J. Fernandez-Baca, G. Alvarez, S. L. Cooper, A. L. Cornelius, and A. Feiguin, *Nanoscale Phase Separation and Colossal Magnetoresistance: The Physics of Manganites and Related Compounds*, Springer Series in Solid-State Sciences (Springer, Berlin, 2003).

[23] M. Y. Kagan and K. I. Kugel, Inhomogeneous charge distributions and phase separation in manganites, Phys. Usp. **44**, 553 (2001).

[24] J. Kim, C. Ko, A. Frenzel, S. Ramanathan, and J. E. Hoffman, Nanoscale imaging and control of resistance switching in VO_2 at room temperature, Appl. Phys. Lett. **96**, 213106 (2010).

[25] S. D. Ha, Y. Zhou, C. J. Fisher, S. Ramanathan, and J. P. Treadway, Electrical switching dynamics and broadband microwave characteristics of VO_2 radio frequency devices, J. Appl. Phys. **113**, 184501 (2013).

[26] Y. Zhou, X. Chen, C. Ko, Z. Yang, C. Mouli, and S. Ramanathan, Voltage-triggered ultrafast phase transition in vanadium dioxide switches, IEEE Electron Device Lett. **34**, 220 (2013).

[27] J. Leroy, A. Crunteanu, A. Bessaudou, F. Cosset, C. Champeaux, and J. C. Orlianges, High-speed metal-insulator transition in vanadium dioxide films induced by an electrical pulsed voltage over nano-gap electrodes, Appl. Phys. Lett. **100**, 213507 (2012).

[28] S. Zhang, M. A. Kats, Y. Cui, Y. Zhou, Y. Yao, S. Ramanathan, and F. Capasso, Current-modulated optical properties of vanadium dioxide thin films in the phase transition region, Appl. Phys. Lett. **105**, 211104 (2014).